Surface morphology, contact size and contact geometry effects on grease-lubricated fretting contacts

David Philippon, Soha Baydoun, Siegfried Fouvry

D. Philippon, S. Baydoun, S. Fouvry, Surface morphology, contact size and contact geometry effects on grease-lubricated fretting contacts, Wear 522 (2023) 204687

(https://doi.org/10.1016/j.wear.2023.204687)

Surface morphology, contact size and contact geometry effects on grease-lubricated fretting contacts

David PHILIPPON(++), Soha BAYDOUN, Siegfried FOUVRY*

Ecole Centrale de Lyon, LTDS Laboratory, 36 av Guy de Collongue, 69130 Ecully, France

*corresponding author: siegfried.fouvry@ec-lyon.fr

(++) Current address: Univ Lyon, INSA Lyon, CNRS, LaMCoS, UMR5259, 69621 Villeurbanne, France (david.philippon@insa-lyon.fr)

Abstract

The fretting behaviour of AISI 52100 steel and low alloy steel under grease lubricated conditions is investigated. The friction behaviour is characterized by a high friction regime for the smallest displacement amplitudes below and next to the partial-slip transition whereas a low friction regime is stabilized above a threshold sliding amplitude when a lubricating tribofilm is generated in the interface. In order to quantify the influence of different contact parameters like surface roughness, contact size and contact geometry, a new fast simplified fretting methodology is introduced. This method allows scanning the entire fretting regime through a single experiment. An experimental comparison of smooth and rough surfaces shows that the effect of surface roughness influences the stability and the performance of the lubricating tribofilm. Experimental results obtained through changing the contact size of the cylinder-on-flat configuration permit identifying two contact size regimes. For small interfaces, the effective fretting sliding amplitude triggering the tribofilm activation is proportional to the contact size, whereas for large contacts this amplitude appears to be constant. The comparison with a punch-on-flat interface suggests that the lubrication activation is better captured by considering the peak pressure width rather than the nominal contact size.

Keywords: Fretting; grease; lubrication; contact size; contact geometry; surface roughness

Nomenclature

a (µm) : half contact width,

b (µm) : half width of the peak pressure,

E (GPa) : elastic modulus,

Ed(J) : friction energy dissipated during a fretting cycle,

f : tangential force ratio (Q*/P),

$\bar{f}$: averaged tangential force ratio over the last 500 fretting cycles,

L(mm) : lateral width of the contacts,

ΔN : increment of fretting cycles during the variable displacement, method,

N : applied fretting cycles,

P (N) : normal force,

P_L(N/mm) : linear normal force per unit of contact length,

p_0 (MPa) : maximum peak pressure,

Q* (±N) : tangential force amplitude,

Q^*_t (±N) : tangential force amplitude at the partial slip / gross slip transition,

R (mm) : radius of the cylinder shape (cylinder-on-flat contact) or radius of the punch border (punch-on-flat contact),

$Rp_{0.2}$ (MPa) : yield stress at 0.2% plastic deformation,

Rm (MPa) : maximum stress

greek symbols

δ (µm) : imposed (measured) displacement,

δ* (±µm) : displacement amplitude,

δ^*_t : displacement amplitude at the partial slip /gross slip transition,

δ^*_{lub} : displacement amplitude where the friction coefficient reaches $\mu_{lub,}$

δ^*_s (±µm) : sliding amplitude,

$\delta^*_{s,lub}$: effective sliding amplitude related to the tribofilm lubrication,

Δδ* (µm) : increment of displacement amplitude during the variable displacement method,

µ : coefficient of friction,

μ_t : coefficient of friction at the partial slip /gross slip transition,

μ_{lub} : coefficient of friction related to tribofilm lubrication (low friction plateau),

1. Introduction

Fretting is an oscillatory motion with small amplitude that occurs between contacting surfaces. The response may be produced by external vibration or cyclic loadings. Using lubricants like grease is one of the mitigations for preventing fretting damage like wear or fretting crack initiation. Lubrication allows relative movement between contacting surfaces but with a lower friction coefficient. Many authors have investigated the impact of different parameters like surface finishing, oil viscosity and its boundary lubrication properties, displacement and frequency amplitude, contact pressure and contact geometry [1-9]. They concluded that the main difference between the alternating and ordinary sliding motion (pin-on-disc, etc.) can be defined in the outlet region where the reverse movement may result in oil starvation. Fretting as oscillatory motion with small amplitudes and very low velocity (even at high frequencies) leads to the situation when dynamic fluid lubrication during sliding is intractable. Fretting regimes under lubricated conditions were first presented in the pioneering work of R.B. Waterhouse's research group in [5] and [6]. They showed that the effect of lubrication on fretting depends on lubricant's ability to penetrate into the contact zone, recover if squeezed out of it, form a boundary film and to reduce the oxygen access. The rate of replenishment of oxygen at the surface is proportional to the diffusivity of the lubricant, which is approximately inversely proportional to viscosity. One of the first investigations examining the effects of deliberately added oils during fretting tests is presented in [6] where high carbon bearing steel was tested using ball-on-flat configuration. Results revealed that lower viscosity oils were able to infiltrate and remain in the fretting contact zone or they were less effective at forming an oxygen shield, so that the oxide layers on the contact surfaces were replenished. Liu et al. [9] showed the maximum value of the friction coefficient for higher viscosity oils was higher and decreased slower than that in lower viscosity ones. This implies that using a low viscosity lubricant allows easier oxygen access and penetration into the interface. No significant decrease in the incubation period

with low friction coefficient was observed. Needless to say, the oxygen access to the contact for lubricated conditions is greatly reduced, so the oxidation of detached particles and worn surfaces decreases and the contact adhesion increases resulting in a higher maximum value of the friction coefficient. Zhou et al. in [8] discussed oil lubricants in fretting and focussed on the competition between the self-cleaning and the self-repairing actions of fretting. They concluded that such competition has to be associated not only with the mechanical parameters of fretting but also with the lubricant properties. Baker et al. performed direct observations of fretting wear on steel under lubricated conditions (sapphire used as a counter body) [10]. The wear coefficient is smaller for the steel-on-sapphire tests compared with the steel-on-steel tests. This could be due to the lower adhesion expected between steel and sapphire compared with steel and steel contact, and its consequent effect on the formation, and perhaps the morphology, of the “primary” (i.e. not yet oxidized) wear particles. The different behaviour of the glass-metal, then metal-metal contact makes the in-situ oil thickness observations hard to interpret and correlate with real steel-steel contacts.

As illustrated in Figure 1, the friction coefficient evolution of a grease-lubricated contact subjected to fretting sliding is highly dependent on the displacement amplitude imposed [9]. For small displacement amplitudes, the stabilized friction coefficient increases with the displacement amplitude. After a threshold amplitude related to the transition from partial to gross slip, the stabilized friction value decreases until reaching a very low friction value related to the complete establishment of a lubricating tribofilm in the interface.

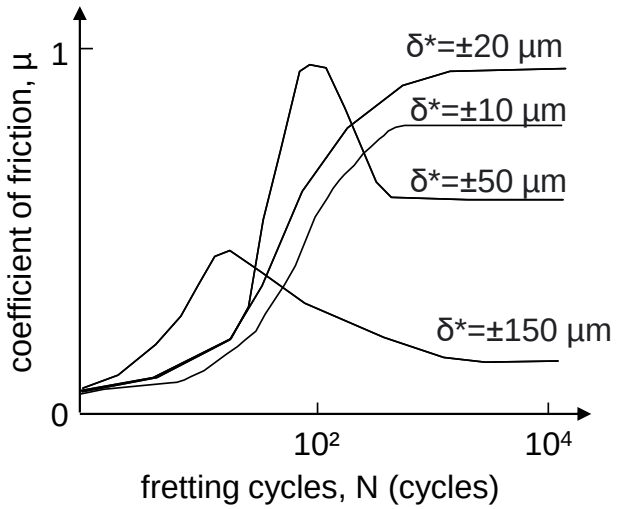

Figure 1: Illustration of the friction coefficient evolution versus fretting cycles under grease lubrication: impact of the displacement amplitude (after [9]).

Such an evolution is obviously dependent on the grease viscosity, boundary lubrication properties, and penetration. It also depends on the contact properties (geometry and contact size) and surface roughness. One major difficulty to complete such an investigation is the huge number of fretting tests required. The purpose of this research work is to provide an experimental strategy to better investigate such specific contacts focusing on the following questions:

- How can the grease-lubricated fretting interface be quantified using a fast reliable variable displacement amplitude test procedure?

- How can the contact size and contact geometry affect the grease-lubricated fretting behaviour?
- How can the surface roughness modify the lubricating tribofilm formation?

2. Experiments

2.1. Test configuration

Fretting tests were performed on a tension compression hydraulic actuator (Figure 2a) which is customized to investigate different contact configurations [11]. The experiments consist in applying a constant normal force (P) while imposing an alternating displacement (δ). The latter is recorded along with the tangential force (Q) and the normal force throughout the test. The evolution of the tangential force versus displacement allows tracing the fretting cycles (Figure 2b). For each cycle, the

maximum tangential force amplitude (±Q*) and displacement amplitude (±δ*) are recorded. Then the friction coefficient μ (Q*/P) is calculated. Thus, the friction coefficient can be monitored during the test.

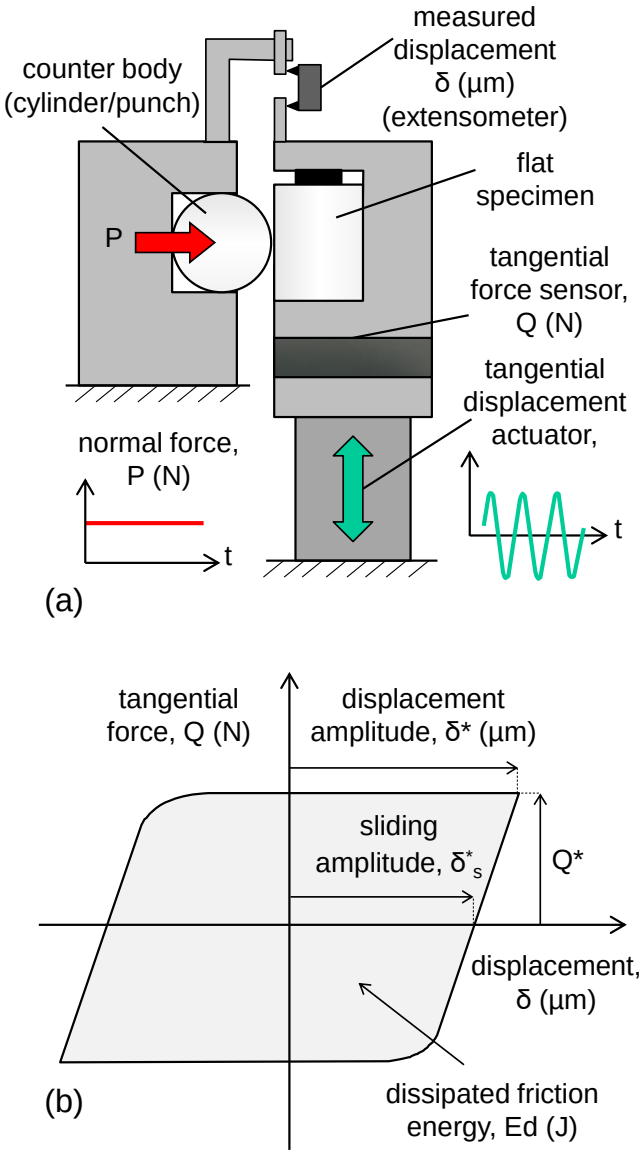

Figure 2: (a) Fretting rig; (b) quantitative variables extracted from a gross slip fretting cycle.

All the tests were conducted under ambient conditions at 25°C with a relative humidity varying between 35 and 45%. The frequency of the sliding oscillations is 5 Hz. The displacement amplitude can be varied from ±0.5 to ±150 μm with a specific displacement control.

Constant but also variable displacement amplitudes can be imposed. Lubricants were smeared with a brush onto both surfaces in contact before applying the normal force. Before smearing with grease lubricant, each sample was cleaned with ethanol. All the tests were repeated at least two times.

2.2. Materials

2.2.1. Flat specimens

Flat specimens (14x12x12 mm^3) were manufactured from a cast tube of low alloy steel (see properties in Table 1 and Table 2). A first group of flat specimens were polished with abrasive paper, finished with diamond paste (3 µm) then cleaned with ethanol. The surface roughness obtained is about Ra = 0.05 µm. The second group of flat specimens was shot peened, leading to Ra = 4.1 ± 0.2 µm surface roughness.

Table 1: Chemical composition of the studied materials

Element (%at.) / Material	C	Mn	Cr	Ni	Ti	Cu	Si	P	S	Mo	V
Low alloy steel	0.43	1.9	-	0.25	-	0.35	0.45	0.03	0.03	-	-
AISI 52100	1.1	0.4	1.6	0.4	1.1	1.1	0.35	0.025	0.025	0.1	0.3

Table 2: Mechanical properties of the studied materials

Material	Hardness	Young's modulus E (GPa)	Poisson Coefficient v	$Rp_{0.2}$ (MPa)	Rm (MPa)	A (%)
Low alloy steel	230 HV	206	0.29	606	698	28
AISI 52100	590 HV	210	0.29	1700	2000	-

2.2.2. Counter body

To assess the impact of the contact geometry and contact size on the fretting behaviour, two counter-body geometries have been investigated. Cylinder pads consisting of an AISI 52100 chromium steel (Table 1 and Table 2) ball bearing with a surface roughness around Ra = 0.05 µm have been applied. Various cylinder radii from R=10 to 60 mm have been applied to address the Hertzian contact size effect. The second counter body is a punch (Figure 3) made with the same materials as the flat specimens. The pad surface roughness obtained after machining is Ra = 0.7 µm.

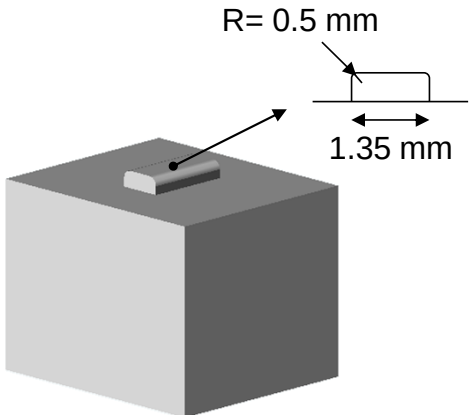

Figure 3: Diagram of the punch geometry sample.

2.2.3. Lubricant (grease)

The study is performed on a commercial grease “Lubrifilm Cleanwell H7S” containing some anti-wear additives like zinc dithiosphosphate (ZnDTP). Indeed, an EDX analysis shows the presence of sulphur, calcium and silicon. Dry and lubricated contacts have been tested. The viscosity of this grease is lower than 7 cSt (mm^2/s) at 40°C. This lubricant has been chosen so that a methodology to characterize the lubricating properties under fretting conditions can be determined.

2.3. Contact configuration

2.3.1. Cylinder-on-flat configuration

The aim of this article is to measure the effect of the contact geometry, contact size and surface morphology on a lubricated fretting contact. To investigate the contact size effect, a cylinder-on-flat geometry is used. Different cylinder radii adjusted with various normal forces are tested so that a single maximum Hertzian pressure p_0 = 540 MPa is applied (Figure 4). For technical aspects, the cylinder counter bodies with a radius lower than 60 mm are tested using a low load specimen holder whereas the 80 mm radius cylinder counter bodies and punch pad specimens are aligned using a high load fretting setup.

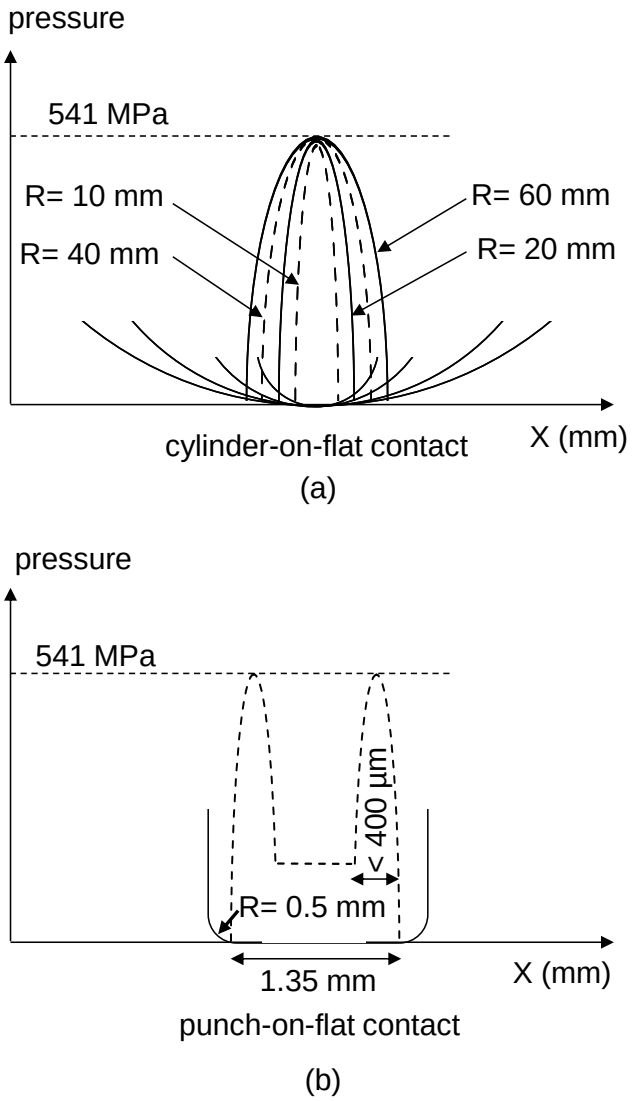

Figure 4: Pressure profiles in a cylinder-on-flat and a punch-on-flat contact ("a": half contact width; "b": half width of the peak pressure).

Elastic loading conditions are imposed permitting the application of Hertzian formulations. The corresponding normal force to achieve the required maximum pressure p_0 is expressed by [12]:

$$P_L = \frac{p_0.\pi.a}{2} \quad (1)$$

Where P_L is the linear normal force per unit of contact length [N/m] and "a" is the half contact width:

$$a = \frac{2.p_0.R}{E^*} \quad (2)$$

With R the cylinder radius and E^* the equivalent modulus expressed by:

$$\frac{1}{E^*} = \frac{1-\upsilon_1^2}{E_1} + \frac{1-\upsilon_2^2}{E_2} \quad (3)$$

E_1 and E_2 are the Young moduli of the plane and the cylinder respectively and v_1 and v_2 are the Poisson's ratio of the flat and cylinder specimens respectively. Table 3 compiles the applied loading conditions for the studied cylinder geometries.

Table 3: Loading and Hertzian parameters for the different cylinder radii.

Radius of the cylinder R (mm)	Maximum pressure p_0 (MPa)	Normal force P (N)	Linear normal force P_L (N/mm)	half contact width *a* (µm)	Lateral contact length L (µm)	Ratio characterizing the 2D plane strain hypothesis a/L
10	540	240	80	94	3000	0.031
20	540	640	160	188	4000	0.047
40	540	1598	319	377	5000	0.076
60	540	2877	479	565	6000	0.094
80	540	5114	639	754	8000	0.094

A 2D plane strain hypothesis is considered. To verify this assumption, the lateral contact length is adjusted so that the half contact width "a" is significantly smaller than the lateral contact width "L" (i.e. the "a/L" ratio remains smaller than 0.1) [11,12].

2.3.2. Punch-on-flat configuration

In addition to the contact size effect, the influence of the contact geometry is investigated by applying a punch equivalent flat with a rounded corner pad (Figure 3). Finite Element Analysis (F.E.A.) computations are performed to adjust the normal loading in order to reach a similar p_0 = 540 MPa maximum peak pressure. As shown in Figure 4b, this configuration induces a typical pressure profile with two maximum peaks at the contact edges bordering a lower inner pressure domain. Each pressure peak is narrower than 400 µm which, compared to the 5 mm punch lateral length, still complies with a 2D plane strain hypothesis.

3. Analysis under constant displacement amplitude conditions

3.1. Evolution of the friction behaviour

Experiments have been conducted on a smooth greasy interface, using a 40 mm radius cylinder-on-flat contact. Figure 5 compares the tangential force ratio $f = Q^*/P$ for three displacement conditions. It is important to mention that under large gross

slip sliding conditions, the tangential force ratio is identical to the friction coefficient (μ=f), while under small displacement amplitudes, partial slip conditions prevail and this identity is no longer satisfied (μ≠f). Therefore, to clarify the discussion, we consider the variable f (tangential force ratio= Q^*/P) assuming that when gross slip conditions prevail the latter variable is equal to the coefficient of friction.

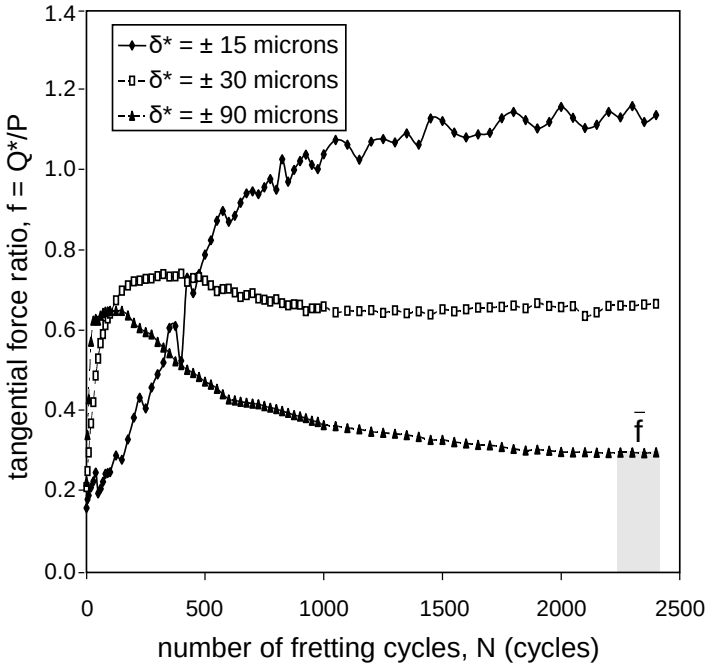

Figure 5: Evolution of the tangential force ratio (f) as a function of fretting cycles for different displacement amplitudes.

The observed evolutions are consistent with the literature [5,8]. The smaller amplitude (i.e. $\delta^* = \pm 15$ μm) is characterized by an initial sharp increase of the tangential force up to a stabilized high friction value f = 1.1. The contact here is running under partial slip conditions. A larger displacement amplitude (i.e. $\delta^* = \pm 30$ μm) promotes a gross slip condition characterized by an elevated stabilized friction value μ=f=0.7. For very large displacement conditions (i.e. $\delta^* = \pm 90$ μm), the friction behaviour is also characterized by an initial sharp increase of the friction coefficient up to 0.7. However, after a short transient period below 1000 cycles, the friction coefficient drops to a very low friction value, stabilizing at μ=f=0.3. To quantify the steady state friction behaviour, a stabilized tangential force ratio, averaged over the last 500 cycles of the test, has been considered.

$$\bar{f} = \frac{1}{N_A}\sum_{i=N-N_A}^{N} f_i \text{ with } N_A = 500 \quad (4)$$

A global overview of the experiments suggests that the chosen duration of 500 cycles appears long enough to extrapolate a reliable description of the steady state friction response. The stabilized tangential value was determined for various displacement conditions. The evolution is drawn in Figure 6. As expected, the shape of the friction curve under greased lubricated condition is consistent with previous studies [7, 9]. The tangential force ratio rapidly reaches a maximum ($\mu_t = f_{max}$), and then it decreases and stabilizes at a lower value (μ_{lub}). Above a threshold amplitude (δ^*_t), the higher the displacement, the lower the tangential force ratio. Taking into account previous investigations [5-6, 8-9, 13], this evolution is related to the formation of a semi-solid lubricating tribofilm. At low amplitudes (partial slip), grease cannot penetrate into the interface. By contrast, high amplitudes inducing gross slip conditions promote grease penetration into the contact.

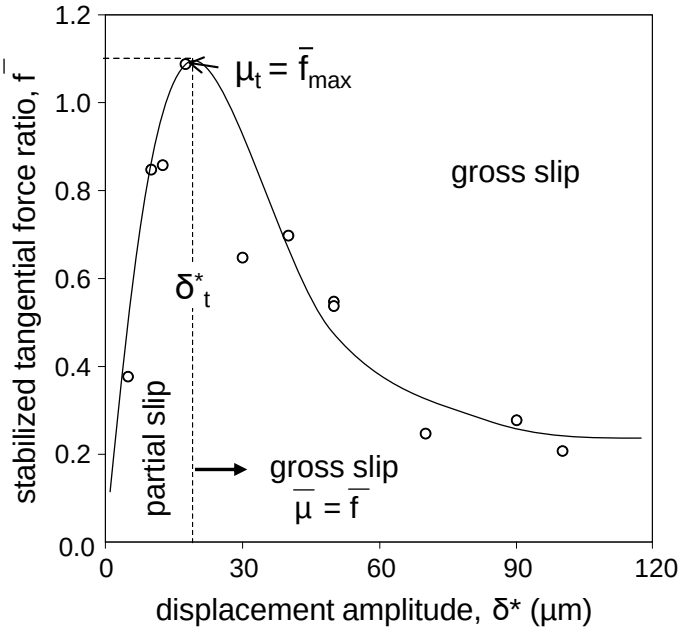

Figure 6: Evolution of the stabilized tangential force ratio (i.e. stabilized friction coefficient for gross slip conditions).

3.2. Analysis of the lubricating tribofilm

One hypothesis to explain the friction evolution versus the displacement amplitude is the formation of a low friction tribofilm within the interface. In order to identify the

distribution of this tribofilm within the interface, optical, SEM and EDX analyses were performed on two representative low and high sliding amplitude conditions, respectively δ^* = ±12,5 µm and δ^* = ±90 µm. This analysis was carried out after ultrasonic ethanol cleaning in order to fully remove the grease from the interfaces. To localize the tribofilm in the fretting scar, one strategy is to follow the EDX iron concentration profile across the fretting scar. If a tribofilm is formed and maintained at the surface, we can assume that the steel substrate will be hidden, inducing a decrease of the iron concentration.

As shown in Figure 7a, below the threshold amplitude δ^*_t (i.e. $\delta^* < \delta^*_t$), partial slip conditions prevail, inducing close fretting loops and a composite interface displaying an inner sticking zone bordered by lateral sliding domains.

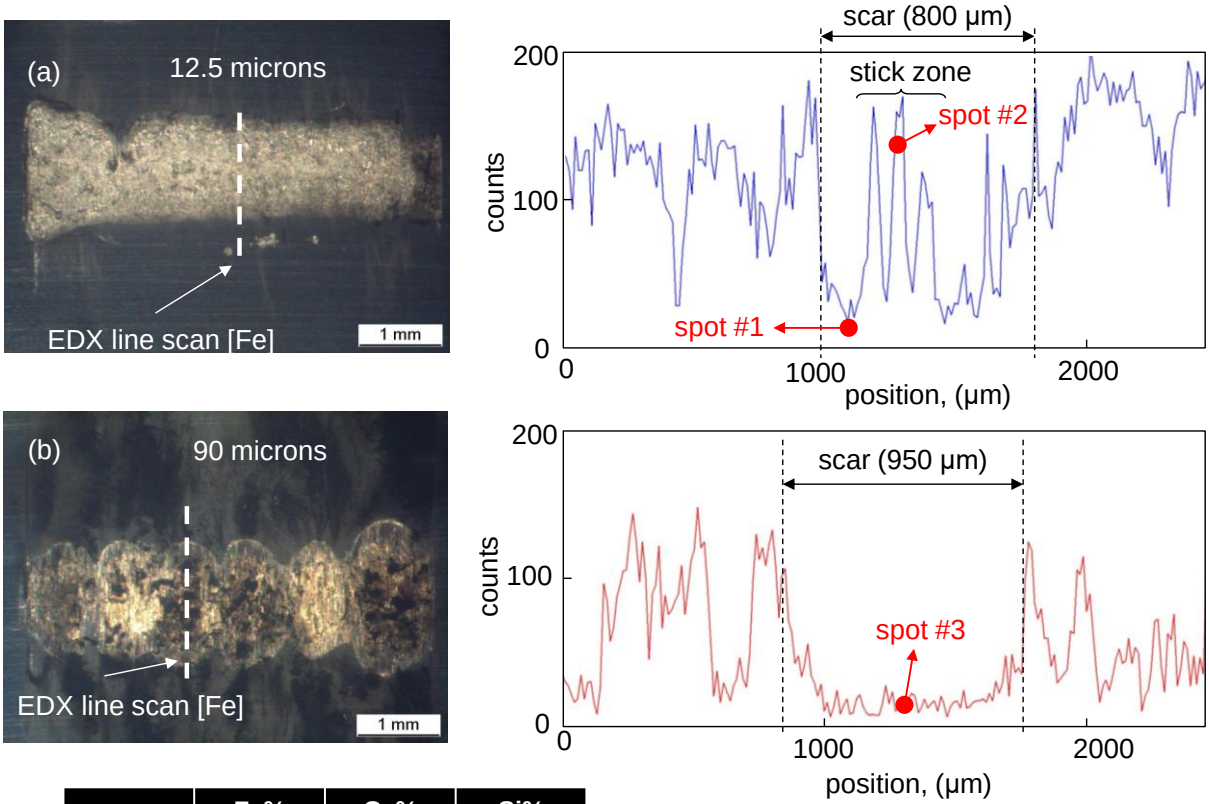

(c)

	Fe%	Ca%	Si%
spot #1	81	12	7
spot #2	89	6	5
spot #3	68	22	12

Figure 7: Fretting scars and EDX iron concentration line scans obtained for: (a) low partial-slip displacement amplitude (δ*= ±12.5 µm) and (b) high gross-slip displacement amplitude (δ*=±90 µm).

The iron profile across the fretting scar (Figure 7a) confirms the composite structure of the partial slip interface. It shows a low number of counts of iron on the lateral edges of the fretting scar but a higher number in the central sticking zone. EDX spot

analyses were done in the zones 1 and 2 (Figure 7a and 7c). The relative composition of Fe (steel surface), Ca and Si (lubricant) is given. A small increase of iron (+7%) and a decrease of calcium (-5%) is noted. This result is consistent with the idea that without any relative sliding the central sticking domain cannot allow the activation of a tribofilm. The iron concentration is therefore equivalent to that detected outside the interface. By contrast, on the external sliding domain, the small sliding amplitude applied seems sufficient to promote the generation of a tribofilm, partly masking the iron signal emerging from the bulk. Above the threshold amplitude, under established gross slip conditions (characterized by a quadratic fretting loop), a heterogeneous fretting scar is observed (Figure 7b). Large quantities of “black” debris inside and also outside the interface can be distinguished. The EDX profile shows a homogeneous low iron concentration within the interface, which suggests tribofilm generation over the whole fretted surface. This is confirmed by the EDX spot analysis (Figure 7c, spot #3) where the relative iron composition decrease and calcium and silicon ones increase. These first analyses confirm the assumption that the friction is controlled by the activation of a lubricating tribofilm. This activation is monitored by the application of sufficient relative sliding within the interface. More in-depth analytical investigations should be undertaken to better characterize the structure of this tribofilm. However, it is not the purpose of this research work which mainly focuses on the geometrical and contact loading aspects.

4. Introduction of a fast fretting test methodology

4.1. Description of the fast methodology

The conventional method usually applied to investigate a lubricated interface consists in performing each test using fixed displacement amplitude. This implies a huge number of experiments. In this article, a new fast methodology is presented where the lubricant effect can be assessed through a single test. This experimental strategy, referred to as “variable displacement method”, consists in increasing the displacement amplitude gradually during the test (Figure 8) and analysing the friction behaviour on-line. At the beginning of the test, the amplitude of increments ($\Delta\delta^*$) is limited to 2.5 µm, then, for higher displacement amplitudes under gross slip conditions, the increment amplitude is increased up to 10 µm. A minimum number of cycles (ΔN) is imposed during each displacement increment in order to stabilize the

interface (ΔN = 1500 cycles). The friction coefficient is recorded at the end of each stabilized step and then drawn as a function of the applied amplitude (Figure 8). The test has been conducted with a 40 mm radius cylinder-on-flat contact.

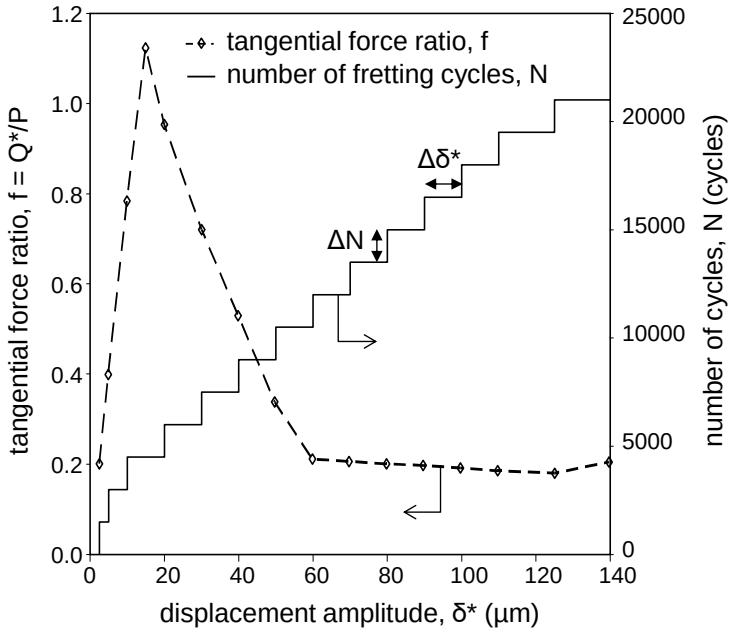

Figure 8: Illustration of the "variable displacement method" (lubricated contact, cylinder-on-flat geometry, R=40 mm, and p_0= 540 MPa).

As confirmed by Figure 9, this fast methodology provides stable and pertinent results compared to the conventional constant amplitude method. The greatest advantage of the variable displacement method is its capacity to describe the whole lubricant behaviour using a single test.

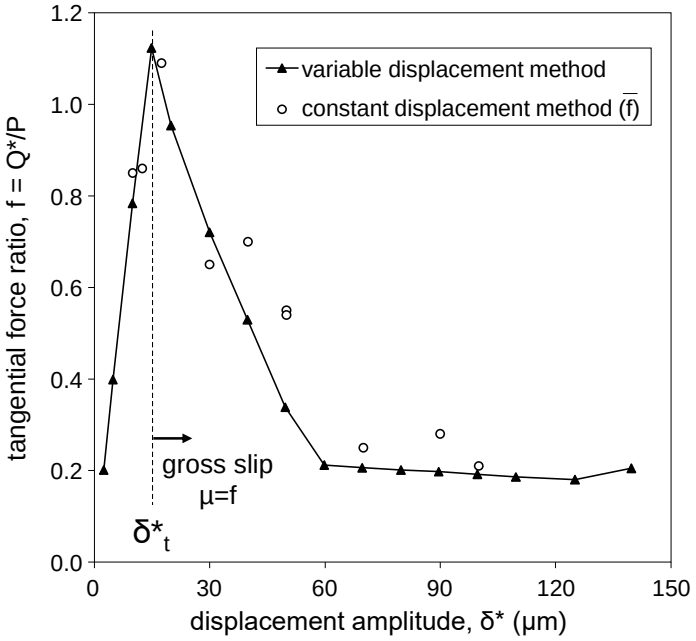

Figure 9: Comparison between conventional tests (Figure 6) and the fast "variable displacement method" (Figure 8) to characterize the friction response under lubricated fretting conditions (R=40 mm and p_0= 540 MPa).

4.2. Fretting sliding behaviour

As previously mentioned, the sliding condition is a key aspect to assess the friction response of the lubricated fretting contacts. To quantify the partial to gross slip transition, an energy sliding ratio A = Ed/Et, with Ed being the dissipated energy (i.e. area of the fretting loop) and Et the total energy ($Et = 4.Q^*.\delta^*$), is considered [11]. The sliding transition is related both to a discontinuous evolution of the ratio A and to a constant At = 0.2 for the sphere-on-flat configuration [13]. Figure 10 shows that the maximum tangential force ratio is reached at the sliding transition which is associated with the discontinuity of the ratio A. For the studied cylinder-on-flat configuration, an experimental threshold can be approximated near At = 0.15. This result confirms previous conclusions regarding the tribofilm formation. Under partial slip conditions, grease cannot fully penetrate the interface and the tangential force ratio is very high. Just after the gross slip transition, the lubricant can infiltrate the interface, activating a tribofilm which promotes a decrease of the friction value (the higher the gross slip amplitude, the lower the friction, until a stabilized low friction value is reached).

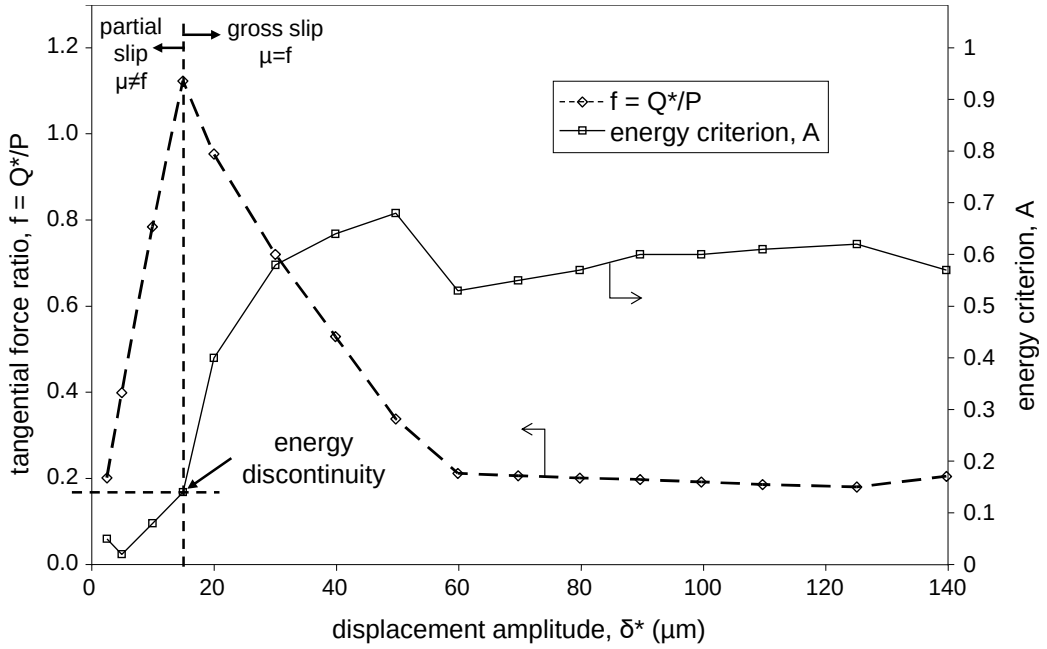

Figure 10: Evolution of the tangential force ratio and the energy ratio A as a function of the displacement amplitude.

This quantitative analysis of the sliding condition confirms the former hypothesis developed by Zhou et al. [8], suggesting that the transition from bad to good lubrication conditions is controlled by the sliding transition, at least for contacts like sphere-on-flat and cylinder-on-flat configurations.

4.3. Definition of quantitative parameters formalizing the lubricated fretting contact

Quantitative parameters to compare the lubricated contact have been defined according to the shape of the curve (Figure 11). δ^*_t is the transition amplitude where the friction coefficient reaches a maximum value $\mu_t = f_{max}$. δ^*_{lub} is the critical amplitude where the friction coefficient reaches a plateau (μ_{lub}). The critical amplitude δ^*_{lub} is a function of the relative sliding within the interface but also includes the contact and test system elastic accommodation. Therefore, to better approximate the actual sliding value, we introduce an effective sliding variable ($\delta^*_{s,lub}$) expressed as the difference between δ^*_{lub} and δ^*_t :

$$\delta^*_{s,lub} = \delta^*_{lub} - \delta^*_t \quad (5)$$

A lubricant will be beneficial when μ_t, μ_{lub}, δ^*_t, δ^*_{lub} and $\delta^*_{s,lub}$ are the lowest. These parameters will be used to quantify the behaviour of a lubricant for a given contact.

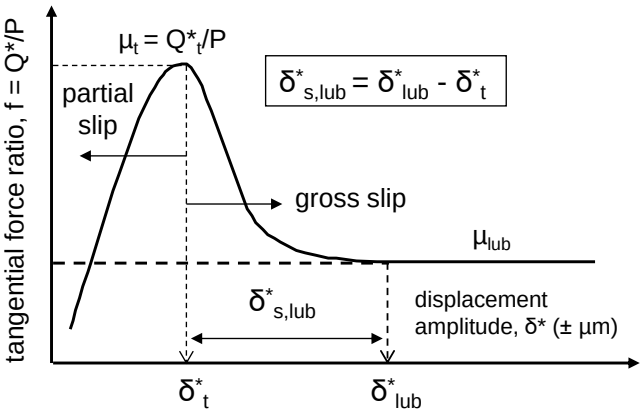

Figure 11: Definition of the quantitative parameters describing the lubricated interface under fretting conditions.

5. Impact of contact parameters on the lubricated interface

5.1. Effect of surface roughness

Surface roughness plays a critical role in tribological processes. To investigate the surface roughness effect in grease lubricated fretting conditions, variable displacement tests were conducted on two surfaces which were radically different in terms of roughness. A shot peened flat specimen was compared with a smooth surface. The morphology of the studied surface is recalled in Table 4 and illustrated by Figure 12.

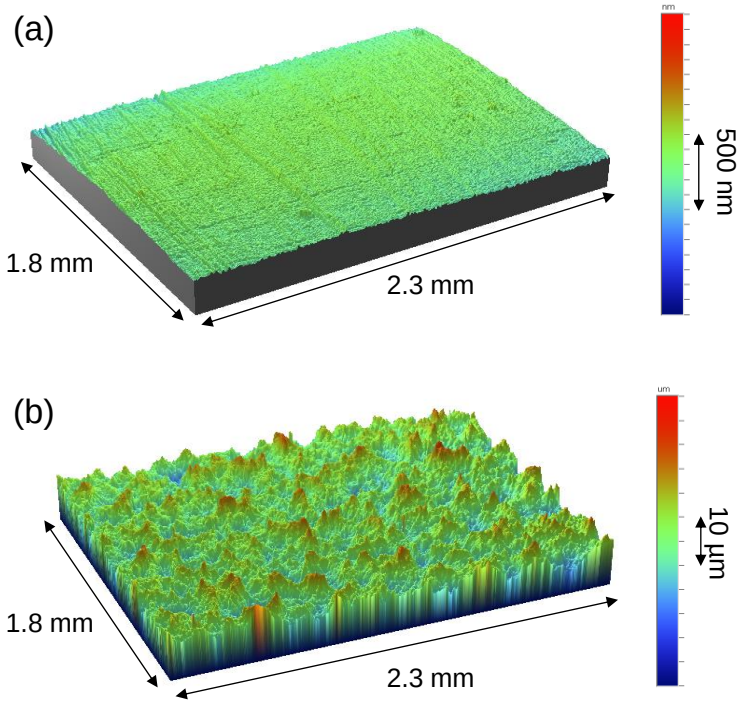

Figure 12: Surface morphology of (a) untreated steel and (b) shot peened surface.

Table 4: Roughness parameters.

Surface	Ra	Rq	Rz	Rt
Untreated	53 nm	66 nm	517 nm	690 nm
Shot peened	4.1 µm	5.2 µm	35.6 µm	41.6 µm

Similar experimental conditions were applied (R=40 mm and p_0=540 MPa). Figure 13 compares the friction evolution of the polished and shot peened specimens under dry and greased conditions. The corresponding quantitative parameters are compiled in Table 5. A rough surface induces a larger δ^*_t value which can be explained by a higher elastic accommodation of asperities (i.e. surface asperities promote more compliant interface than smooth surfaces). However, the effective sliding amplitudes remain stable ($\delta^*_{s,lub}$ = 45 µm), which implies that the critical amplitude δ^*_{lub} is longer for rough surfaces.

Differences regarding the friction values are notable. First of all, the roughness is beneficial under low amplitude conditions. It decreases the friction peak observed at the transition amplitude. The asperities induced by the peening treatment favour oxygen penetration but also the grease retention through the interface. For higher amplitudes, when the lubricant film process is activated, the roughness effect is detrimental. The friction coefficient increases for the shot-peened surface and stabilizes later, at 0.32 instead of 0.21. The asperities of shot peened surfaces induce local over-stressing, inhibiting the formation of a homogenous lubricant film. To confirm this hypothesis, optical imaging (Figure 14) and EDX analyses (Figure 15) were made on the fretting scars. Figure 15a represents the number of counts of iron elements inside and outside the scar of untreated and peened surfaces. As previously mentioned, when the number of counts is important, it suggests that the lubricant tribofilm thickness is negligible. This is confirmed by EDX spot analyses showing the relative iron (steel substrate), calcium and silicon (grease). On the peak (spot #2), iron increases compared to the value of the plateaus (spot #1 and spot #3) whereas calcium and silicon decrease. This means that the zones with the iron peaks are not covered by the tribofilm. In the case of the peened surface, some iron peaks can be observed. These peaks correspond to asperities not covered by the tribofilm.

By contrast, the smooth surface displays a homogeneous low iron signal within the fretting scar which suggests the presence of a homogeneous lubricant tribofilm.

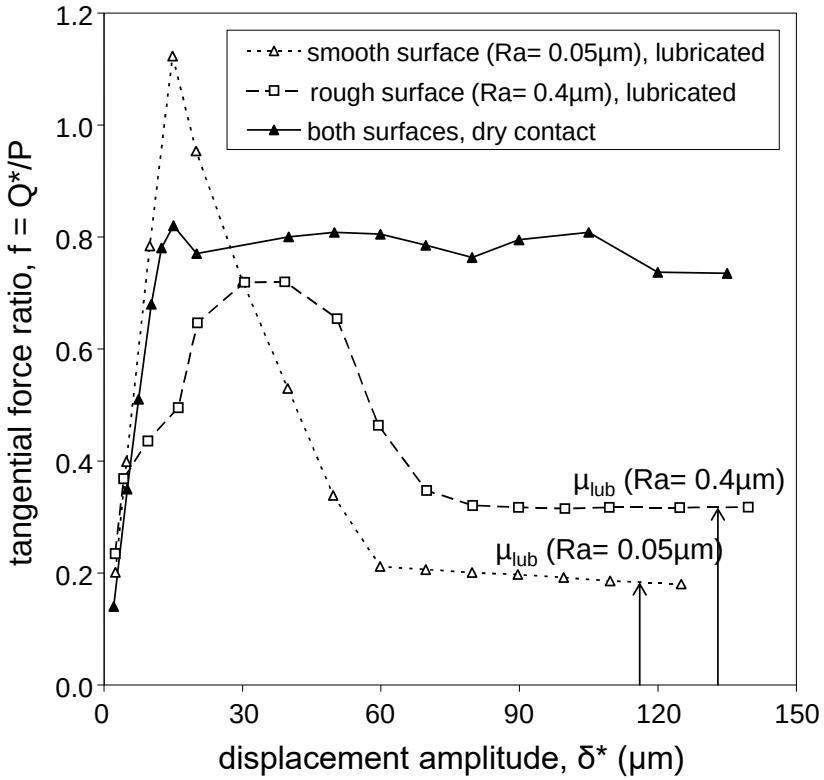

Figure 13: Evolution of the friction behaviour as a function of the applied displacement amplitude with different surface roughness.

Table 5: Quantitative parameters extracted from the experimental analysis (Figure 13) describing the friction behaviour under greased fretting conditions.

Surface state	Smooth (Ra=0.05 µm)	Rough (shot peened) (Ra=4 µm)
δ^*_t	15	35
δ^*_{lub}	60	80
$\delta^*_{s,lub}$	45	45
μ_t	1.12	0.72
μ_{lub}	0.21±0.01	0.32±0.07

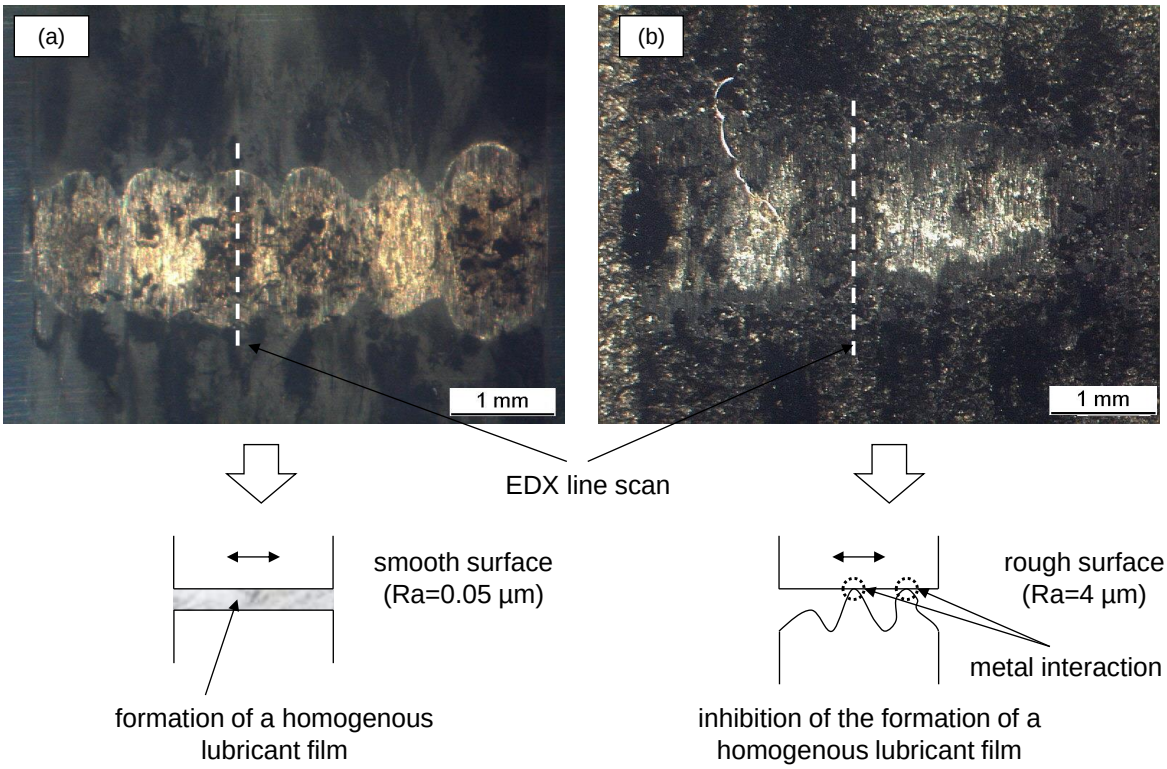

Figure 14: Optical observations and schematic illustration of the contact under large displacement amplitudes as a function of the surface roughness: (a) shot peened surface: $\delta^* = \pm 85$ µm and (b) smooth surface: $\delta^* = \pm 90$ µm.

Note that the given fretting sliding analysis is associated with the global contact size dimension (i.e. macro contact size). Considering the analysis at the asperity scale (Figure 14), a local “reciprocating” sliding description should be preferred since the applied sliding amplitude e.g. 20 µm is significantly longer than the asperity dimension (i.e. less than 10 µm). However, insofar as the contact is never exposed to the external environment, the concept of “non-exposed asperity reciprocating sliding” is probably more representative.

(a)

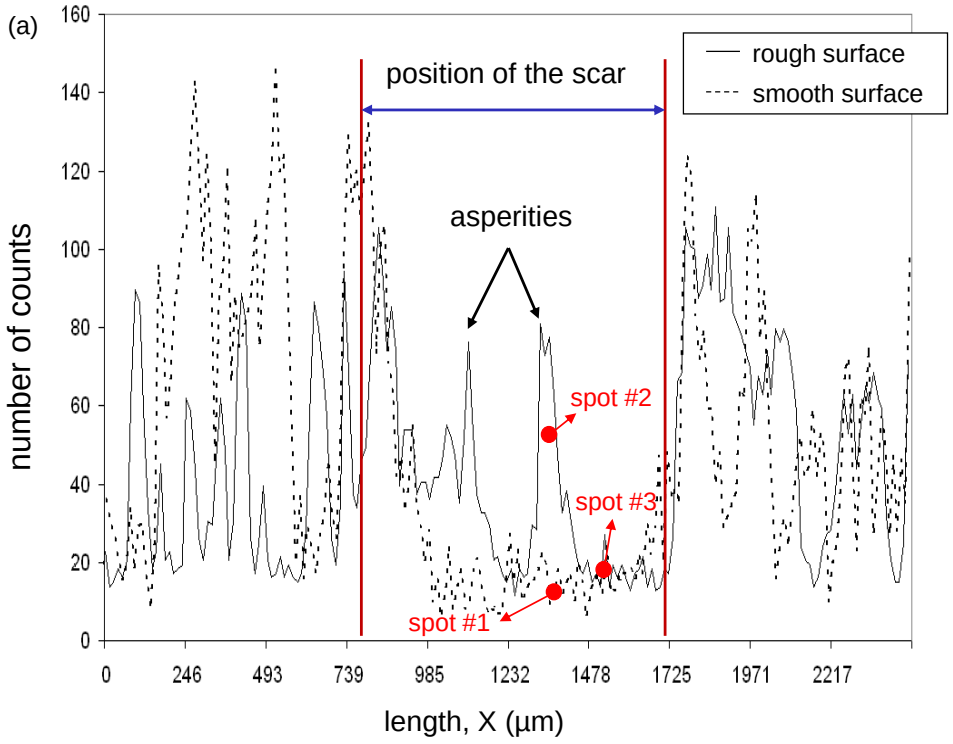

(b)

	Fe%	Ca%	Si%
spot #1 (smooth surface)	66	22	12
spot #2 (smooth surface)	78	12	10
spot #3 (rough surface)	53	21	20

Figure 15: EDX (a) line scans and (b) spot analyses of the scar displaying distribution of iron across the fretting scar of rough and smooth surfaces.

5.2. Contact size effect

Zhou et al. [8] hypothesized that the effectiveness of grease lubrication depends strongly on the ratio of the slip amplitude to the contact size. They found that this palliative efficiency increases with this sliding ratio. These hypotheses were made and checked in the case of sphere-on-flat configuration. The same hypothesis can be made for a cylinder-on-flat contact, but in this case, the contact size is not the most important parameter, but rather the contact width “2a” (Figure 16). An original experimental procedure consisting in imposing various contact sizes, while maintaining a constant maximum pressure p_0=540 MPa, is applied (Figure 4, Table 4).

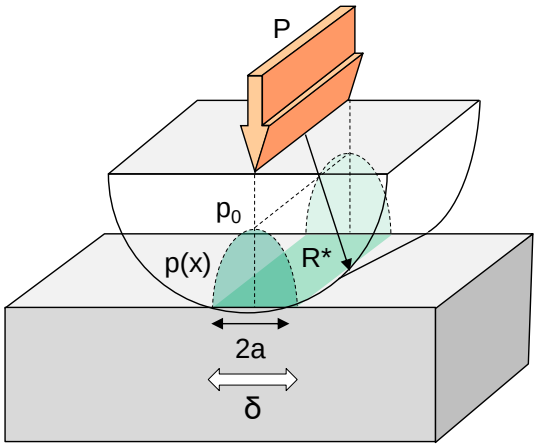

Figure 16: Illustration of the pressure profile in a cylinder-on-flat interface.

The characteristic friction curves obtained for the different contact size configurations are plotted in Figure 17.

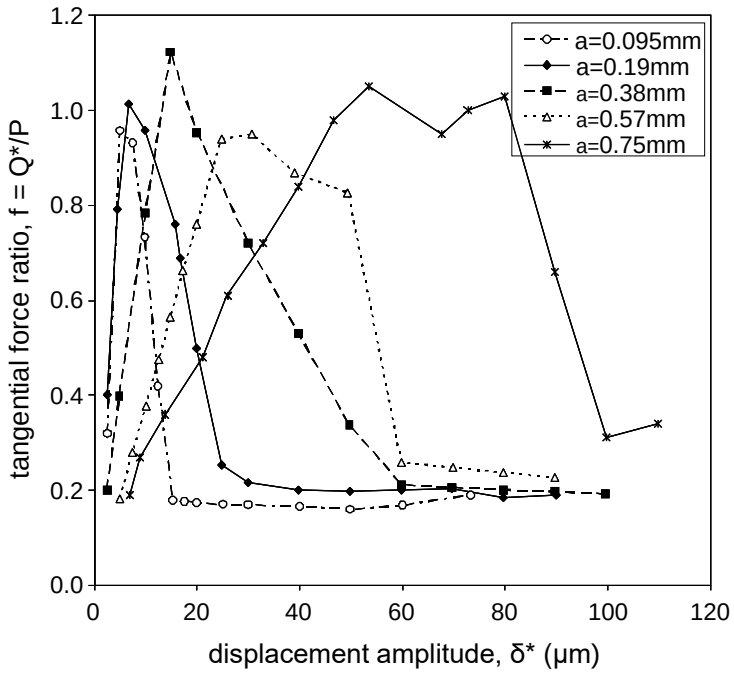

Figure 17: Evolution of friction behaviour for different contact sizes (p_0=540 MPa).

The quantitative parameters, defined by averaging 3 duplicated tests, are compiled in Table 6. δ^*_{lub} and δ^*_t are shown to be highly affected by the contact size. When the contact size increases, both δ^*_{lub} and δ^*_t increase. Figure 18 displays the evolution of the δ^*_t/a ratio versus the corresponding half contact width “a”.

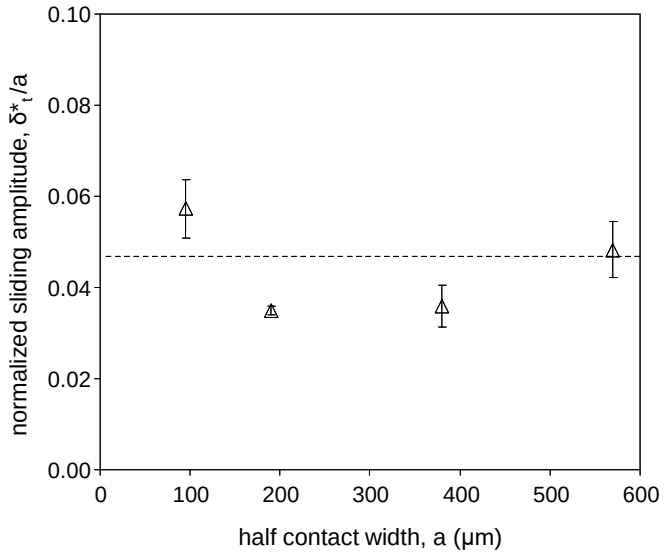

Figure 18: Evolution of the δ^*_t /a ratio as a function of the Hertzian half contact width (cylinder-on-flat configuration, R ≤60 mm and p_0 = 540 MPa).

The δ^*_t/a ratio remains nearly constant whatever the contact size. This is consistent with the Mindlin's theory of dry contacts (as sphere-on-flat configurations) stating that δ^*_t is proportional the contact size "a" [12, 13]. On the other hand, this suggests that under partial slip condition, the mechanical response of a greased interface is equivalent to a dry contact. This result indirectly supports previous experimental research studies [5-7] underlying that as long as a greased fretting contact operates under partial slip, its tribological response is equivalent to a dry contact.

Now focusing on the gross slip domain, to better quantify the lubricant film formation, it appears more suitable to consider the effective sliding amplitude ($\delta^*_{s,lub}$) rather than the displacement amplitude since this latter is highly affected by the test system compliance. Figure 19a suggests a discontinuous evolution of $\delta^*_{s,lub}$ versus the half contact width. Below a threshold contact size ($a_{th} \approx 400$ µm), the effective sliding amplitude requested by tribofilm activation tends to increase linearly with the Hertzian half contact width. Above this threshold, the effective sliding amplitude stabilizes at a constant value ($\delta^*_{s,lub,th} \approx 40$ µm).

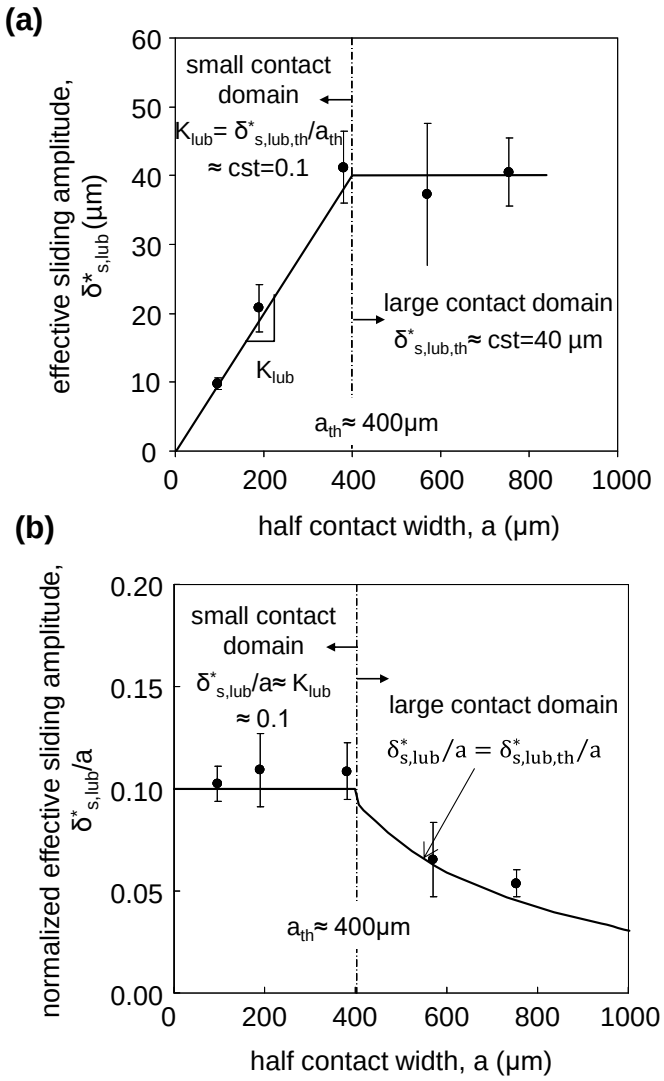

Figure 19: (a) Evolution of the normalized $\delta^*_{s,ub}$ as a function of the Hertzian half contact width of cylinder-on-flat contact ; (b) Evolution of the normalized effective amplitude ($\delta^*_{s,lub}$ /a) as a function of the Hertzian half contact width (Cylinder-on-flat configurations: R= 10, 20, 40, 60, 80 mm, and p_0 = 540 MPa).

By drawing inspiration from the Mindlin's description of δ^*_t transition, it is also possible to describe the lubrication behaviour considering the $\delta^*_{s,lub}/a$ ratio. As illustrated in Figure 19b, the $\delta^*_{s,lub}/a$ ratio remains nearly constant in the small contact size domain (i.e. $a \leq a_{th} \approx 400$ µm) suggesting that the lubricating tribofilm is fully activated if a constant proportion of the fretted interface is spread (i.e. about 10% of the half contact width). Alternatively, for the larger contact sizes (i.e. $a \geq a_{th} \approx 400$ µm), $\delta^*_{s,lub}/a$ ratio decreases asymptotically toward zero. The following relationships are derived:

- If $a \leq a_{th} \approx 400$ µm , $\delta^*_{s,lub} = K_{lub} \times a$

or

$\delta^*_{s,lub}/a = K_{lub}$

with $K_{lub} = \frac{\delta^*_{s,lub,th}}{a_{th}} \approx 0.1$

- If $a \geq a_{th} \approx 400$ µm , $\delta^*_{s,lub} = \delta^*_{s,lub,th}$

or

$\delta^*_{s,lub}/a = \delta^*_{s,lub,th}/a$ (6)

with $a_{th} \approx 400$ µm and $\delta^*_{s,lub,\,th} \approx 40$ µm.

This description of contact size effect introduces the underlying proportional or constant contact size dependence on the tribofilm activation for small and large interfaces respectively. A complete description will require the investigation of a very large contact configuration which cannot be addressed presently due to experimental limitations.

Table 6: Quantitative variables (mean values of three tests) describing the friction behaviour of the cylinder-on-flat configuration ($p_0=p_{max}$=540 MPa).

R: cylinder radius (mm)	10	20	40	60	80
P: normal force (N)	243	648	1620	2915	5150
a: half contact width (µm)	95	191	381	572	754
$\delta^*_{t,}$(µm)	5.4±0.6	6.7±0.2	13.6±1.7	27.5±3.5	54±1.4
δ^*_{lub} (µm)	15.2±0.2	27.4±3.5	54.9±7	64.8±7	94.5±6.3
$\delta^*_{s,lub}$ (µm)	9.7±0.8	20.7±3.4	41.2±5	37.3±10	40.5±5
$\mu_t=\mu_{max}$	0.96	0.96	1.05	0.95	1.08
μ_{lub}	0.17±0.05	0.20±0.10	0.25±0.19	0.25±0.09	0.31±0.09
$\delta^*_{t/a}$	0.06±0.006	0.035±0.001	0.036±0.005	0.048±0.006	0,072±0.002
$\delta_{lub/a}$	0.16±0.002	0.14±0.019	0.14±0.018	0.114±0.012	0.125±0.008
$\delta_{s,lub/a}$	0.10±0.009	0.11±0.018	0.11±0.014	0.065±0.018	0.054±0.007

5.3. Impact of the contact geometry

In addition to contact size effect, it appears interesting to evaluate how the contact geometry can affect the lubricated fretting behaviour. Thus, a typical punch-on-flat geometry (Figure 3), characterized by a non-Hertzian pressure distribution, displaying two maxima of pressure peaks at the contact edges, is investigated. The applied normal force was computed at 1072 N to reach a similar 540 MPa maximum peak pressure. A similar variable displacement methodology was applied to quantify the

friction behaviour. Figure 20 compares both cylinder-on-flat and punch-on-flat friction response under dry and lubricated conditions.

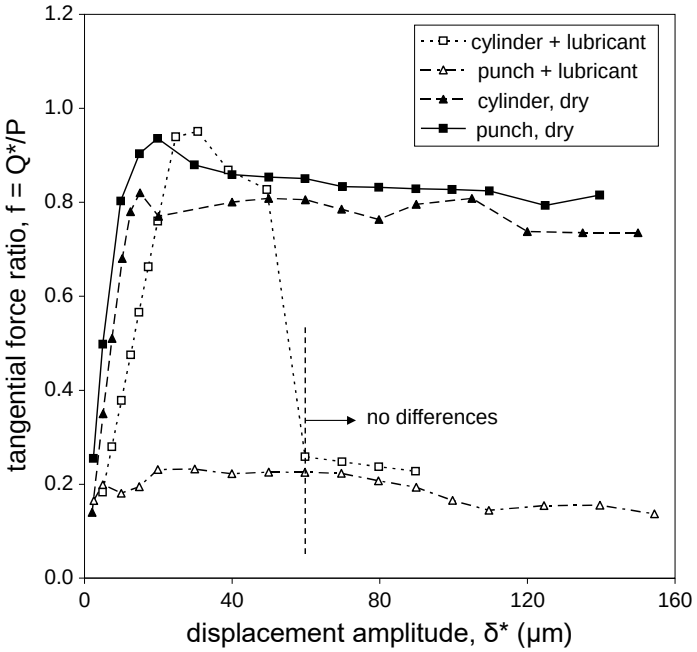

Figure 20: Evolution of the friction coefficient as a function of the applied displacement amplitude, comparison between cylinder-on-flat and punch-on-flat contact geometries (p_0=p_{max}=540 MPa).

Equivalent friction evolutions are observed under dry conditions. This suggests that the friction behaviour of a complex punch-on-flat geometry can be approximated using the simpler cylinder-on-flat configuration, assuming that the contact size is comparable. Considering the lubricated situation, these experimental results show that a similar low friction response is achieved if the applied sliding amplitude is sufficient to activate a stabilized lubricating tribofilm.

By contrast, very large differences are observed in the transient small amplitude domain. For the cylinder-on-flat configuration, the friction displays a peak evolution near 0.9, equivalent to the dry contact. Alternatively, the punch-on-flat configuration displays a quasi-instantaneous activation of the lubricating tribofilm. The maximum friction coefficient during this transient period remains systematically lower than 0.25.

Similar to cylinder-on-flat analysis, the lubricated friction response of the punch-on-flat interface is investigated. The transition amplitude is established at δ^*_t= 20 µm whereas the stabilized low friction regime is observed above a stabilized displacement amplitude δ^*_{lub}= 160 µm. The different quantitative data are compiled in Table 7.

Table 7: Quantitative variables (mean value of three tests) describing the friction response of the lubricated fretting punch-on-flat contact (p_{max} = 540 MPa).

Parameter	Punch-on-flat contact
a: half contact width (µm)	1350
δ^*_t (µm)	20
δ_{lub} (µm)	170
$\delta^*_{s,lub}$ (µm)	150
$\delta^*_{s\ lub}/a$	0.11
μ_t	0.23
μ_{lub}	0.13±0.01

The effective sliding amplitude evolution defining the tribofilm activation is compared in the normalized sliding chart. Figure 21 shows that the punch-on-flat result is not at all consistent with the predicted tendency extracted from the cylinder-on-flat investigation. Although, the half width of the punch contact is very large, the corresponding effective sliding ratio ($\delta^*_{s,lub}/a$) is around 0.1, equivalent to a small cylinder-on-flat configuration. It can be concluded that the contact size description, defined from the Hertzian contact analysis, cannot be transposed to the specific case of a punch-on-flat geometry. These open questions will be addressed in the following discussion.

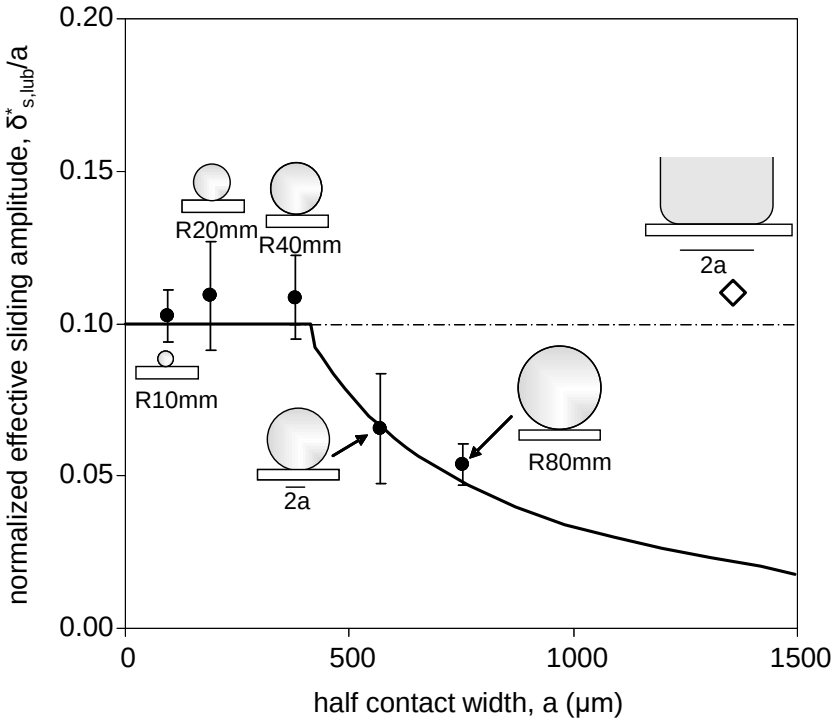

Figure 21: Evolution of the normalized effective sliding amplitude ($\delta^*_{s,lub}/a$) as a function of the half contact width "a" ($p_0 = p_{max}$= 540 MPa, ●cylinder-on-flat (b=a), ◇ punch-on-flat).

5.4. Discussion

This experimental investigation shows that increasing the surface roughness improves lubrication in the small amplitude transient period, favouring oxygen access but also grease conservation within the interface. However, it inhibits the formation of a homogenous lubricating tribofilm for larger sliding amplitudes and consequently increases the friction level of the low friction regime. More interesting results are extracted from the cylinder-on-flat and punch-on-flat contact configurations. The Hertzian cylinder-on-flat configuration is characterized by a maximum pressure located at the middle of the interface. This promotes lubricant ejection outside the interface and can explain why, for the smallest amplitudes, the friction response is similar to a dry interface. Increasing the relative sliding, the lubricant can progressively penetrate below the interface and generate the formation of a lubricating tribofilm [14]. This investigation shows that the effective sliding amplitude allowing the grease feeding and the tribofilm formation is a function of the contact size. It is proportional to the half contact width for the smallest interfaces but converges to a constant value above a threshold contact dimension a_{th}. Obviously, this behaviour and the related constitutive variables will depend on the applied contact pressure and potentially lubricant properties. Further experimental investigations are already planned to investigate these aspects.

The punch-on-flat configuration displays a similar transient period followed by a lower friction regime. However, the very small maximum friction observed suggests that the activation of the lubricant tribofilm is quasi-instantaneous. This can be explained by the typical pressure field imposed. Indeed, the maximum peak pressures are located at each border of the interface. Therefore, unlike the Hertzian interfaces, it can be assumed that a major part of the grease is captured below the interface between the two peak pressures. This favours the incipient activation of the lubricating tribofilm and prevents a severe increase of the friction coefficient even for the smallest displacement amplitudes. However the establishment of a stable and complete lubricant tribofilm requires a critical quantity of grease flow to be transferred from the outside edge of the contact towards the inner domain of the interface, either to regenerate the tribofilm located in the central low pressure domain or to generate a

tribofilm below the peak pressure. This implies that a significant sliding amplitude must be imposed so that the external lubricant will overcome the narrow lateral peak pressure. With this interpretation, it is easier to understand why the punch-on-flat interface corresponds better to a small Hertzian interface (Figure 21). The distance related to the grease transfer, is not a function of the nominal contact width but rather corresponds to the thinner lateral peak pressure zone. Assuming that the transition from small to large contact regime is controlled by the pressure field distribution, it is interesting to plot the normalized sliding ratio ($\delta^*_{s,lub}/a$) versus the half width of the peak pressure "b". Note that for the Hertzian configuration, the peak pressure width is equivalent to the nominal contact size (i.e. b=a). For the studied punch-on-flat contact, the half width of the peak pressure was estimated around b_{punch} = 200µm.
Figure 22 shows that the punch-on-flat result correlates better with the master curve defined from the cylinder-on-flat configuration.

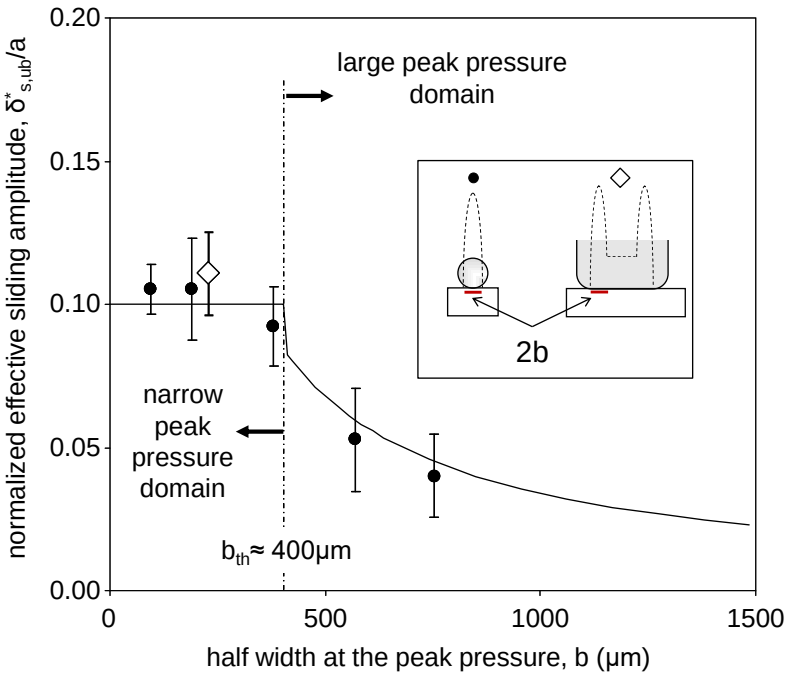

Figure 22: Evolution of the normalized effective sliding amplitude ($\delta^*_{s\_lub}$) as a function of the peak pressure width ($p_0 = p_{max}$= 540 MPa, ●cylinder-on-flat (b=a), ◇ punch-on-flat contact).

This suggests that a synthetic description of the lubrication activation can be made if the length scale parameter used to calibrate the size effect is related to the width of the peak pressure rather than the nominal contact size. Like for the previous description, a threshold width of the peak pressure (b_{th}≈ 400µm) can be identified, dividing the sliding behavior between narrow and large peak pressure configurations.

However, deeper investigations are required to better interpret the relative interactions between the nominal contact width and the peak pressure influence. Indeed, the contact length scale is expressed as a function of the width of the peak pressure whereas the sliding parameter, activating the lubrication, is still expressed as a function of the nominal contact width. On the other hand, this suggests that the sliding parameter describing the contact lubrication process is well described by the $\delta^*_{s,lub}/a$ ratio, but the evolution of the latter parameter seems to be controlled by the half width of the peak pressure "b". This investigation proposes that two different length scale variables "a" and "b" need to be considered to calibrate the tribological response of a grease-lubricated interface subjected to fretting sliding: a first one "a" to capture the capacity of the grease to reach the center of the contact allowing the formation of a homogeneous lubricious tribofilm, a second one "b" illustrating the capacity of the grease to overpass a peak pressure which tends to prevent the extension of this latter toward the inner part of the contact. For Hertzian contact, both "a" and "b" are similar but it is not the case for more complex contact configurations like the studied punch-on-flat contact.

6. Conclusion

An experimental investigation focusing on surface roughness, contact size and contact geometry effects in a grease-lubricated fretting contact was developed. The following conclusions were drawn.

- A fast simplified fretting methodology, referred to as "variable displacement method", was introduced to characterize the grease performance in fretting interfaces.
- A non-monotonic evolution of the friction response of greased interfaces was observed. High friction regime equivalent to a dry contact has been observed under partial slip condition. However, above the sliding transition amplitude, the coefficient of friction displayed an asymptotic decrease until a low and stable friction value when a lubricant tribofilm was formed.
- An effective sliding amplitude variable $\delta^*_{s,lub}$, independent of the test system compliance signature, was introduced to quantify the performance of greases under small gross slip sliding amplitudes condition (i.e. next to the partial slip/ gross slip transition).

- An increase of the surface roughness was shown to reduce the maximum friction value at the sliding transition (δ^*_t) compared to a smooth surface. This can be explained by the higher entrapment and the easier access of the oil lubricant. Nevertheless, by inhibiting the formation of a homogenous lubricating tribofilm, rough surfaces promoted higher friction values (μ_{lub}) under gross slip conditions.
- An original experimental procedure combining different cylinder shape radii was developed to investigate the contact size effect of greased interfaces. Below a threshold contact size a_{th}, the effective sliding amplitude appeared proportional to the contact size but remained constant in the large contact size domain ($a>a_{th}$).
- The tribological response of the greased punch-on-flat geometry was shown to be very different from the Hertzian cylinder-on-flat contact. The constitution of a tribofilm over the whole interface seemed to be activated when the external lubricant is able to overcome the thin lateral peak pressure domain. Thus, it appeared more consistent to compare the sliding response using the peak pressure width “b” than the nominal contact size “a”. A master curve, where the “$\delta^*_{s,lub}/a$” is expressed as a function the peak pressure width “b” is introduced to combine both cylinder-on-flat and punch-on-flat results

Further experimental work will be carried out to confirm the given description and clarify the typical response of punch-on-flat geometry. Combined with modelling aspects, a more physical description of the given experimental results is also expected [15]. Despite some limitations, this first overview also appears as an interesting approach to compare and optimize the structure and the composition of greases and lubricants as mitigations against micro-fretting oscillations.

Acknowledgements

This research did not receive any specific grant from funding agencies in the public, commercial, or not-for-profit sectors.

References

[1] Imai M., Teramoto H., Shimauchi Y., Tonegawa E., Effect of oil supply on fretting wear; Wear 110, 1986: 217-225.

[2] Sato J., Shima M., Sugawara T., Tahara A., Effects of lubricants on fretting wear of steel; Wear 125, 1988: 83-95.

[3] Neyman A., The influence of oil properties on the fretting wear of mild steel; Wear 152 (1), 1992: 171-181.

[4] Qiu Y., Roylance B.J., The effect of lubricant additives on fretting; Lubrication Engineering 48 (10), 1992: 801-808.

[5] I.R. McColl, R.B. Waterhouse, S.J. Harris, M. Tsujikawa, Lubricated fretting wear of a high-strength eutectoid steel rope wire; Wear 185 (1-2) (1995) 203-212.

[6] M. Shima, H. Suetake, I.R. McColl, R.B. Waterhouse, M. Takeuchi, On the behaviour of an oil lubricated fretting contact; Wear 210, 1997: 304-310.

[7] Zhou Z.R., Kapsa Ph., Vincent L., Grease lubrication in fretting; Journal of Tribology 120, 1998: 737-743.

[8] Zhou Z.R., Vincent L., Lubrication in fretting - a review, Wear 225, 1999: 962-967.

[9] Liu Q.Y., Zhou Z.R., Effect of displacement amplitude in oil-lubricated fretting; Wear 239, 2000: 237-243.

[10] Baker, R.F., Olver, A.V., Direct observation of fretting wear of steel; Wear 203-204, 1997: 425-433.

[11] Fouvry S., Duo P., Perruchaut Ph., A quantitative approach of Ti-6Al-4V fretting damage: Friction, Wear and crack nucleation , Wear 257(9-10), 2004:916-929.

[12] Johnson, K.L., Contact mechanics, ed. C.U. Press. 1985.

[13] S. Fouvry, Ph. Kapsa, L. Vincent, "Analysis of sliding behaviour for fretting loadings: determination of transition criteria", Wear 185,1995 : 35-46.

[14] Kalin M., J. Vizintin, S.Novak, G. Drazic, Wear mechanisms in oil-lubricated and dry fretting of silicon nitride against bearing steel contacts, Wear 210 (1997) 27-38.

[15] Lubrecht, A. A., Mazuyer, D., Cann, P., Starved elastohydrodynamic lubrication theory: application to emulsions and greases, Comptes rendus de l'Académie des Sciences - Série IV, 2001 (2, 5):717-728.